The Ionosphere at L Band: MeerKAT

W. D. Cotton (NRAO), J. J. Condon (NRAO), T. Mauch (SARAO) October 9, 2018

***Abstract*—Unusually large artifacts in sensitive imaging of a quiet field using the MeerKAT L band system are traced to ionospheric effects during 6 of the 18 hours of the observations. These caused apparent position shifts of sources which varied with time, frequency and location in the field of view and are not fully corrected by self–calibration. While the corrupting effects are not common in the $\sim$ 100 hours of observations on this field, they are largely at night when ionospheric activity is less than during the day and especially sunrise and sunset. It is speculated that the ionospheric problems are aggravated by the small size of the MeerKAT dishes, hence large field of view. Ionospheric problems are expected to increase as the sun come out of minimum and especially with the lower frequency MeerKAT UHF system.**

***Index Terms*—ionosphere**

I. Introduction

IONOSPHERIC phase effects increase with decreasing frequency and can be very important at low frequencies. Since the ionosphere is several hundred km from the array these effects can range from all sources in the field of view having an apparent common motion on the sky to sources having differential motion to sources being being defocused. Such effects are very common at frequencies below a few hundred MHz but have recently been seen in MeerKAT data at L band (900-1670 MHz). This memo discusses this data as processed in the Obit package [1] [1].

II. Ionosphere vs. Troposphere

The effects of ionospheric phase errors can be quite different from those of tropospheric phase errors as is illustrated in Figure 1. Tropospheric errors mostly come from water vapor which is usually relatively close to the array; typically, all sources in the field of view of a given antenna will have the same effect but the effect will vary from antenna to antenna which will defocus sources in derived images. At microwave frequencies water vapor is "gray" and induces the same excess path length independent of frequency. As shown in Figure 1, a gradient in excess path will cause an apparent position shift; since the length of a baseline in wavelengths goes as ν, the phase effect of the water vapor on a given baseline also goes as ν. Tropospheric effects at microwave frequencies are generally removed by self–calibration.

The ionosphere typically peaks several hundred km above the Earth so all antennas of arrays of a few km in size may see the same phase screen. The excess path induced by the charged particles increases as ν^{-2} so the baseline phase goes as ν^{-1}. There are three regimes of ionospheric effects[2]:

1) **Common motion.** If all antennas effectively look through the same ionospheric phase gradient which is constant across the field of view, all sources will appear to be shifted on the sky, an effect that is time variable as the ionosphere drifts by. Self calibration will completely remove this effect. This case is also described as having an antenna pattern which is smaller than the isoplanatic patch size (size of phase coherence on the sky).
2) **Differential motion.** If all antennas see a given source through the same ionospheric gradient but see different sources through different gradients, there will appear to be differential motions of undistorted sources on the sky in addition to any common motions. Self–calibration will not correct this regime but "Field–based" calibration [3], [4], [2] will.
3) **Defocusing.** If different antennas see the same source through different gradients, the phase effects will be incoherent and the source will be defocused. This is the case of the isoplanatic patch being much smaller than the field of view.

III. Event of 14 Sept. 2018

As part of a program of deep observations of a particularly quiet field ("DEEP_2"), test imaging of the data-set taken on 14–15 September 2018 showed unusually high levels of artifacts around the brighter sources. A closer examination revealed these to be due to an ionospheric disturbance lasting the first six hours of the observation.

A. Observations

The data were collected from 1800 UT on 14 Sept. 2018 through 1200 UT on 15 Sept. 2018 in the MeerKAT L band (900 - 1670 MHz) with 4096 spectral channels, full polarization (linear feeds) and 8 sec integrations. The flux density and band-pass calibrator, 1934-6349, was observed once at the beginning of the run; the delay and phase calibrator J0252-7104 was observed every 15 min for 1 min. The target field was RA=4 13 26.4, dec= +80 0 0. The MeerKAT observation number is 1536948100.

B. Calibration

Data were divided into 8 Spectral Windows with equal numbers of channels to aid in the calibration and imaging. Calibration used the standard MeerKAT/Obit pipeline script using two passes of delay, band-pass and amplitude and phase calibration inter mixed with RFI detection and flagging steps. The spectrum of the phase reference source (8.458 Jy SI=-0.894) was determined relative to the standard spectrum of 1934-638 and the gains for the calibrator source were applied to the target data.

National Radio Astronomy Observatory, 520 Edgemont Rd., Charlottesville, VA, 22903 USA email: bcotton@nrao.edu
South African Radio Astronomy Observatory, Pinelands(?), South Africa
[1]http://www.cv.nrao.edu/∼bcotton/Obit.html

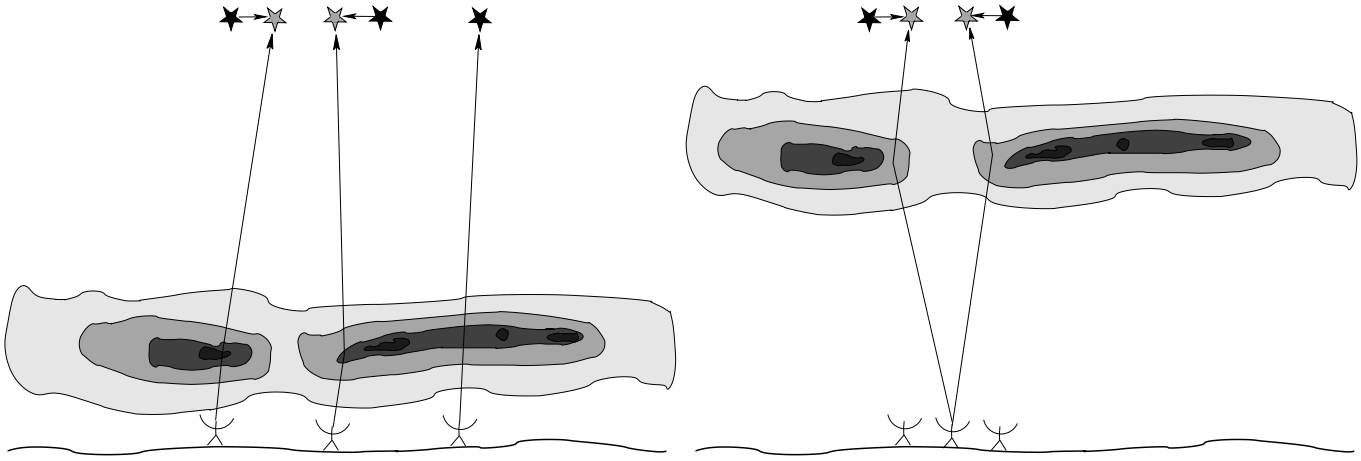

Fig. 1. Cartoons showing the difference between tropospheric phase errors (Left) and those from the ionosphere (Right), figures from [2]. Filled stars give the true position while empty stars are the apparent position. Tropospheric phase errors will defocus sources while ionospheric errors may only appear to move them on the sky.

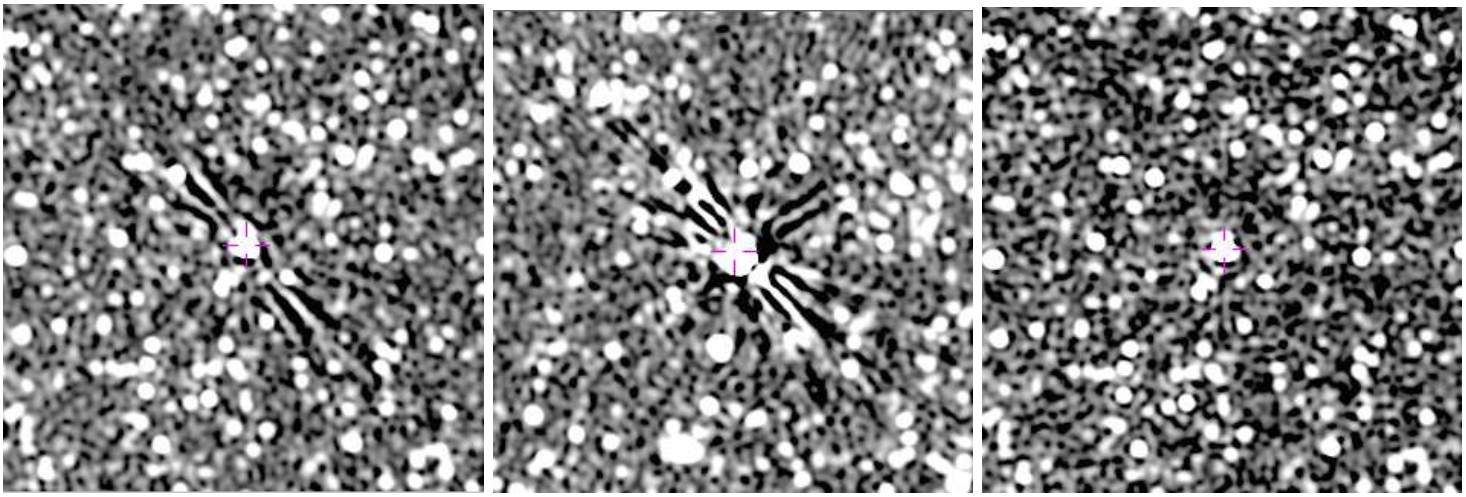

Fig. 2. Regions around bright sources all with the same stretch and after self–calibration. Left and center panels are two sources in different parts of the beam imaged using all data showing different patterns of artifacts. The right panel is the same as the left panel but imaged excluding the first 6 hours of data heavily affected by disturbed phases.

C. Full Synthesis

The initial, test imaging of this data-set using Obit task MFImage including phase self–calibration showed an unusually high level of artifacts around the brighter sources; examples are shown in Figure 2. The details of the artifacts varied with position in the field and appear to be largely antisymmetric (i.e. due to phase errors). This effect plus the fact that self–calibration did not remove these artifacts suggests phase errors varying across the field of view implying an ionospheric effect.

D. Temporal Phase Behavior

These data were imaged using Obit task MFImage which performed one iteration of phase only self–calibration with a 30 sec. solution interval. These solutions are differential corrections to the calibration by J0252-7104. The statistics of the phase solutions including all antennas and both parallel hand polarizations (XX, YY) for each antenna and Spectral Window were determined in 5 min intervals. The average abs(phase) and standard deviation of the phase are plotted for the lowest ($\sim$900 MHz) and highest ($\sim$1500 MHZ) Spectral Windows as a function of time in Figure 3. These plots show substantially higher mean phase residual and scatter for the first 6 hours (until $\sim$0 UTC on 15 Sept 2018) as well as higher mean and standard deviations for the lowest frequencies. This is consistent with an ionospheric disturbance rather than a tropospheric disturbance as the latter should be more prominent at the highest frequency. Imaging with self–calibration of the data-set excluding the first 6 hours largely removes the artifacts as is shown in Figure 2 right in which these artifacts are no longer visible. The artifacts clearly come from the first 6 hours.

E. Snapshot Imaging

As a final test, 5 min snapshot imaging was done around the brightest sources in the field to look for other signatures of ionospheric problems, apparent position shifts varying with time, frequency and location in the field of view (Case 2 in

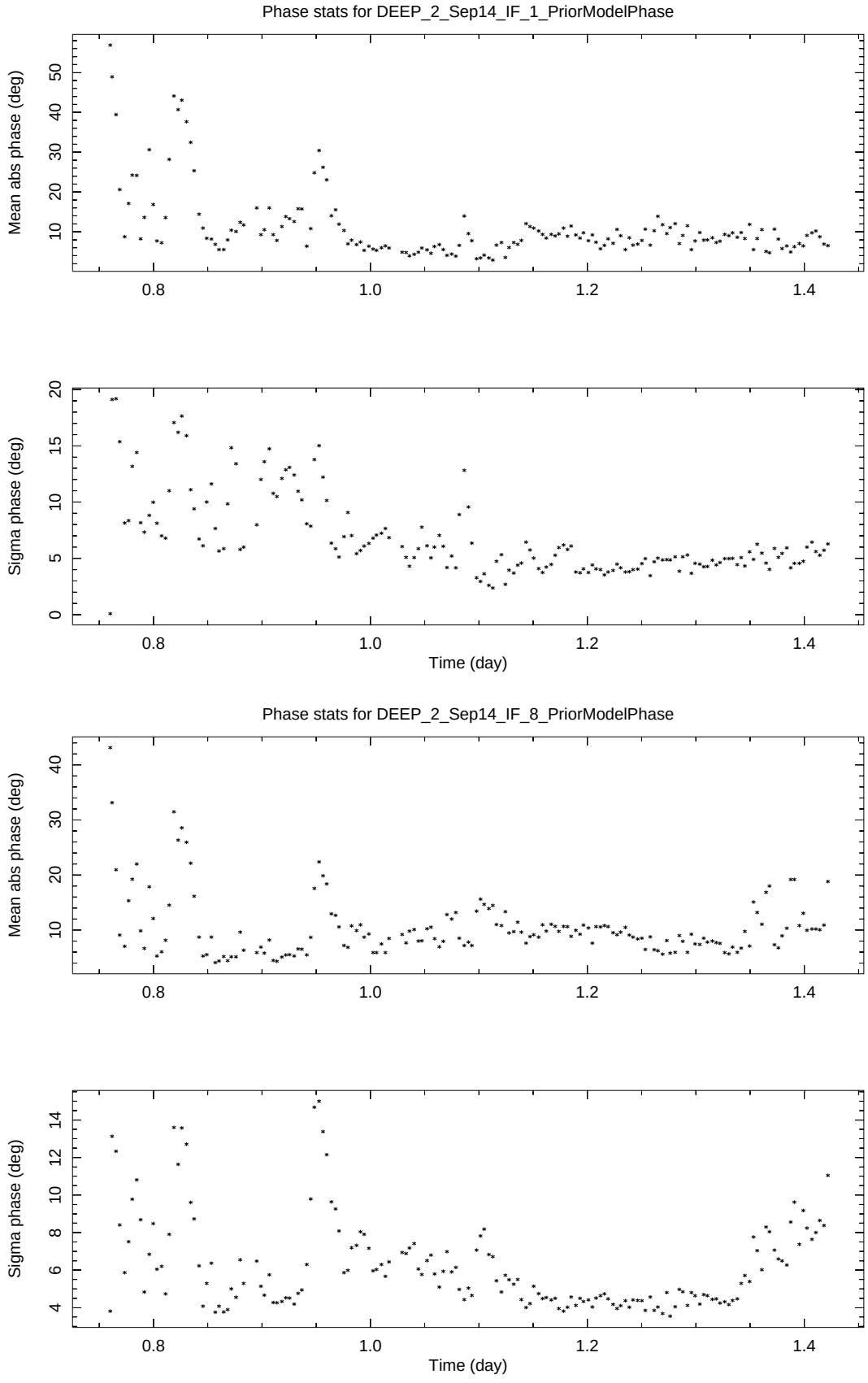

Fig. 3. Mean of abs(phase) and standard deviation of self-calibration solution phases from all antennas as a function of time after external calibration. Upper pair is Spectral Window 1 (∼900 MHz), lower pair is Spectral Window 8 (∼1500 MHz). Zero time is 0 UTC on 14 Sept 2018.

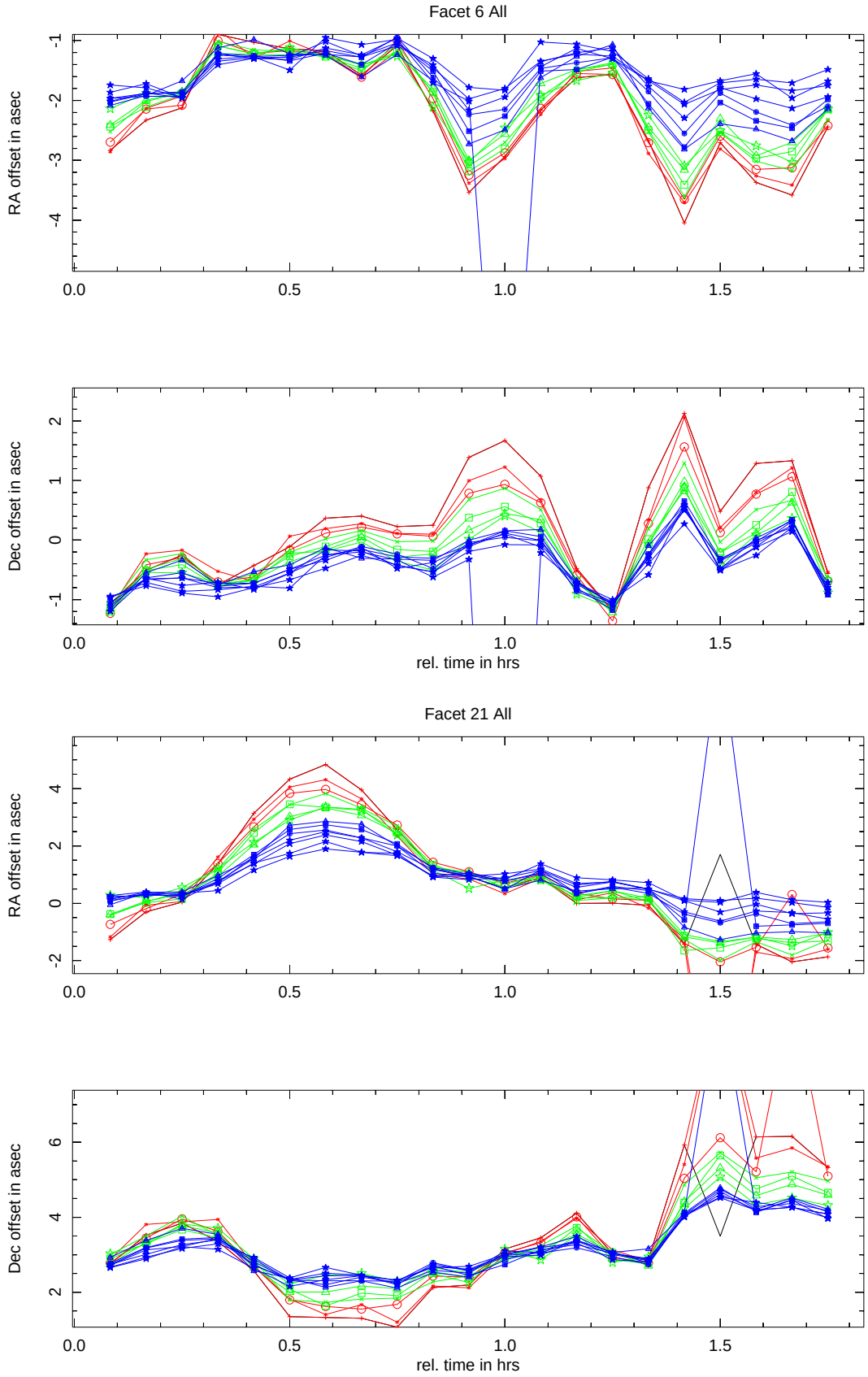

Fig. 4. RA and dec fitted offsets from the expected position as a function of time for sources in two locations of the beam showing different behavior. Different symbols are for different frequency bins and red indicates the lowest frequencies, green, intermediate and blue the highest frequencies. The largest variations are for the lowest frequencies. Source 6 (top) is at 04 00 20.6587 -79 49 2.641 and source 21 (bottom) at 04 18 2.1025 -80 19 31.361.

Section II). MFImage deals with sky brightness and beam variations with frequency of wide fields by dividing the spectrum into bins in frequency narrow enough that variations with frequency inside the bin does not cause significant problems. These frequency bins are imaged independently and jointly CLEANed [5]. In this case the fractional bandwidth in each bin was 0.05 giving 14 bins across the observed band-pass. This field was picked for a lack of bright sources and the sources imaged have peak flux densities 5-25 mJy/bm, hence limited SNR in short time intervals and relatively narrow frequency bins. Plots of the RA and dec offsets as a function of time and frequency of two of the better behaved sources are shown in Figure 4. These two sources are in different positions in the field of view and show very different pattern of apparent motion in time and frequency. Note: pairs of sources close together on the sky show very similar patterns. In addition, the variation in position is stronger at lower frequencies than at higher frequencies. This is the pattern of ionospheric effects commonly seen at lower frequencies [3], [4], [2].

IV. Ionospheric activity

Ionospheric activity (AKA "space weather") affects more than radio astronomy and is constantly monitored by satellites. The Kp index is a measure of global ionospheric activity and the 3 hours averages for 14-15 Sept. 2018 are shown in Figure 5. This figure shows nothing significant during the period 1800 UT on 14 Sept. 2018 through 0 UT on 15 Sept. 2018 during which the MeerKAT observations were affected. There was stronger activity earlier on the 14th and a moderate (G2) geomagnetic storm on Sept. 11. Satellite monitoring appears unable to reliably predict when there is ionospheric activity strong enough to affect radio interferometer data.

V. Discussion

An event causing significant imaging artifacts in sensitive MeerKAT L band observations was traced to ionospheric activity which caused varying differential motion of sources in the field of view with time and frequency (Case 2 in Section II). This effect was unexpected at this frequency as it has never been reported at this frequency with the VLA (WSRT?). However, the MeerKAT antennas are substantially smaller than those of the VLA (and WSRT) and illuminate a field of view roughly twice the linear size of the 25 m antennas.

Roughly 100 hours of observations have been done by MeerKAT on this field and only the 6 hours of 14 Sept data - as indicated by the self–cal residual phase plots - show a problem at the level reported here. However, ionospheric disturbances are more common at sunset and sunrise and the 14 Sept data were the only data on this field taken through sunset.

Ionospheric effects in Case 1 of Section II will be removed by self calibration and would go unnoticed. The effects of a given level of ionospheric activity which are uncorrected by self–calibration should go quadratically with the field of view making MeerKAT more susceptible to these problems than arrays with larger antennas. Since both ionospheric phase errors and field of view vary inversely as the frequency, the MeerKAT UHF system will have this problem far more often and may require calibration/imaging capable of reducing these effects. Solar activity has been unusually low for the past several years of the current solar minimum; when the sun returns to a more normal level of activity, ionospheric disturbances will become stronger and more frequent. Case 3 of Section II (complete defocusing) is not expected at L band. Satellite global ionospheric monitoring showed nothing of note during the MeerKAT event.

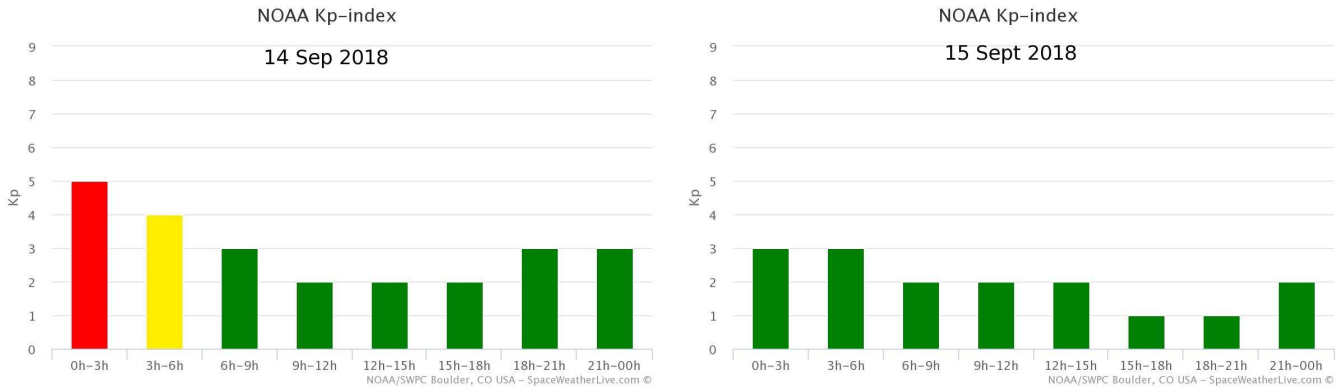

Fig. 5. Satellite global ionospheric activity Kp index for 14 Sept. 2018 (left) and 15 Sept. 2018 (right). Source: https://www.spaceweatherlive.com/

REFERENCES

[1] W. D. Cotton, "Obit: A Development Environment for Astronomical Algorithms," *PASP*, vol. 120, pp. 439–448, 2008.

[2] W. D. Cotton, J. J. Condon, R. Perley, N. Kassim, J. Lazio, A. Cohen, W. Lane, and B. Erickson, "Beyond the Isoplanatic Patch in the VLA Low Frequency Sky Survey," *SPIE*, vol. 15489, pp. 180–189, 2004.

[3] W. D. Cotton and J. Uson, "Ionospheric Effects and Imaging and Calibration of VLA Data at 327 MHz," *EVLA Memo Series*, vol. 117, pp. 1–12, 2007. [Online]. Available: ftp://ftp.cv.nrao.edu/NRAO-staff/bcotton/Obit/Ion327.pdf

[4] W. D. Cotton, "Ionospheric Effects and Imaging and Calibration of VLA Data," *EVLA Memo Series*, vol. 118, pp. 1–12, 2007. [Online]. Available: ftp://ftp.cv.nrao.edu/NRAO-staff/bcotton/Obit/IonImage.pdf

[5] Cotton, W. D., J. J. Condon, K. I. Kellermann, M. Lacy, R. A. Perley, A. M. Matthews, T. Vernstrom, D. Scott, and J. V. Wall, "The Angular Size Distribution of μJy Radio Sources," *ApJ*, vol. 856, p. 67, 2018.